12

AD A125530

AD

MEMORANDUM REPORT ARBRL-MR-03249

DYNAMIC RESPONSE OF THE HEMISPHERICAL CONTAINMENT STRUCTURE SUBJECTED TO TRANSIENT LOADS AT THE R-9 FIRING RANGE

Aaron D. Gupta
Henry L. Wisniewski

March 1983

US ARMY ARMAMENT RESEARCH AND DEVELOPMENT COMMAND
BALLISTIC RESEARCH LABORATORY
ABERDEEN PROVING GROUND, MARYLAND

Approved for public release; distribution unlimited.

UNCLASSIFIED

SECURITY CLASSIFICATION OF THIS PAGE (When Data Entered)

REPORT DOCUMENTATION PAGE

READ INSTRUCTIONS BEFORE COMPLETING FORM

1. REPORT NUMBER: MEMORANDUM REPORT ARBRL-MR-03249
2. GOVT ACCESSION NO.: AD-A125 530
3. RECIPIENT'S CATALOG NUMBER:
4. TITLE (and Subtitle): DYNAMIC RESPONSE OF THE HEMISPHERICAL CONTAINMENT STRUCTURE SUBJECTED TO TRANSIENT LOADS AT THE R-9 FIRING RANGE
5. TYPE OF REPORT & PERIOD COVERED: FINAL
6. PERFORMING ORG. REPORT NUMBER:
7. AUTHOR(s): Aaron D. Gupta; Henry L. Wisniewski
8. CONTRACT OR GRANT NUMBER(s):
9. PERFORMING ORGANIZATION NAME AND ADDRESS: US Army Ballistic Research Laboratory, ATTN: DRDAR-BLT, Aberdeen Proving Ground, MD 21005
10. PROGRAM ELEMENT, PROJECT, TASK AREA & WORK UNIT NUMBERS: 1L162618AH80
11. CONTROLLING OFFICE NAME AND ADDRESS: US Army Armament Research & Development Command, US Army Ballistic Research Laboratory (DRDAR-BL), Aberdeen Proving Ground, MD 21005
12. REPORT DATE: March 1983
13. NUMBER OF PAGES: 38
14. MONITORING AGENCY NAME & ADDRESS (if different from Controlling Office):
15. SECURITY CLASS. (of this report): UNCLASSIFIED

15a. DECLASSIFICATION/DOWNGRADING SCHEDULE:

16. DISTRIBUTION STATEMENT (of this Report): Distribution unlimited, approved for public release.
17. DISTRIBUTION STATEMENT (of the abstract entered in Block 20, if different from Report):
18. SUPPLEMENTARY NOTES:
19. KEY WORDS (Continue on reverse side if necessary and identify by block number):
Blast pressure
Containment structure
Dynamic response
Finite difference
Firing Range
20. ABSTRACT (Continue on reverse side if necessary and identify by block number)

Large deflection elastic-plastic response of a 9m radius hemispherical containment shell structure .0254 m thick clamped to a horizontal rigid foundation and subjected to explosive blast loading due to a 29.03 Kg TNT charge at the center was analysed using a finite-difference structural response code, i.e., PETROS 3.5. The hemispherical enclosure is the most stress-critical structure in the R-9 firing range located at the Spesutie Island.

DD FORM 1 JAN 73 1473 EDITION OF 1 NOV 65 IS OBSOLETE

UNCLASSIFIED

SECURITY CLASSIFICATION OF THIS PAGE (When Data Entered)

The peak reflected overpressure was estimated from a scaled distance of the wall from the point of detonation based on a conservative cube-root scaling law. The reflected overpressure decay with time was assumed to obey the modified Friedlander equation. The residual quasi-static overpressure was obtained from an equation developed by Kinney and Sewell based on the ratio of the available vent area and the internal volume.

Only a quarter segment of the structure was modelled using 18 equal width meshes in one layer and four Gaussian integration points through the thickness in each mesh. The 1020 steel was represented by a trilinear curve followed by a perfectly-plastic behavior and elastic-plastic unloading resulting in a polygonal approximation.

The results indicated the initiation of flexural waves at the clamped edge propagating towards the pole and thereby altering the spherically symmetric breathing mode of response of the structure. The peak deflection was predicted by the code to occur at the pole and permanent displacement after releasing the load was found to be quite small. Transient strain components at the inner and outer surfaces near the clamped edge due to mainly elastic oscillations showed significant bending deformation. In conclusion, the protective structure was found to be an efficient configuration capable of safe containment of internal explosive blast loading.

TABLE OF CONTENTS

LIST OF ILLUSTRATIONS

I. INTRODUCTION

A. Background

The Ballistic Research Laboratory is currently in the process of acquiring a target enclosure to facilitate destructive terminal ballistic testing of chemical explosives (CE), armor and kinetic energy (KE) penetrators by safe containment of blast, fragments and resultant combustion products. The present investigation is based on a preliminary concept of the firing range as shown in Figure 1. The target is located inside the hemispherical enclosure at the end of a long concrete pipe-guide. The gun-launched projectile travels through the pipe-guide and enters the enclosure through a .914 m diameter hole. The target interaction with the projectile is monitored photographically with flash X-ray equipment, and penetration velocity is obtained using velocity screens and electronic counters. An air exhaust system mounted at the rear of the structure operates during the test and draws back aerosolized material out of the enclosure after a test and traps it in filters in the exhaust ducting. A large sliding door with a configuration to match the curvature of the hemispherical wall allows equipment access inside the enclosure. The door is sealed to the wall with a pressurized hose seal along its perimeter. The entire structure is built to contain blast and fragments, to trap aerosolized materials and to permit photographic observation of the test.

A significant problem associated with the enclosed range tests is the overpressure resulting from shock loading as well as rapid heating of the air within the enclosure as the penetrator and the target are torn apart during their encounter as shown by R. Abrahams et al.[1] The structure must survive both the reflected and the residual overpressures induced by the interaction until ambient conditions are reached due to venting out to the atmosphere through the exhaust system.

B. Objectives

Since the key element of the AHKELS (Advanced High Kinetic Energy Launch System) range is the enclosure structure, The Blast Dynamics Branch was assigned to estimate the overpressure loading on the wall and analyze dynamic response of the preliminary configuration at critical locations and assure structural integrity from a conservative viewpoint. The choice of a hemispherical configuration was influenced by an earlier investigation by N. J. Huffington et al.[2] who demonstrated the effectiveness of such a protective structure.

In the absence of any available experimental data, it was decided to obtain a theoretical estimate of the transient and residual overpressure loading due to a centrally located equivalent charge weight at the base. The

---

[1] *R. Abrahams, R. Peterson, and B. Bertrand, "Measurement of Blast Pressure Produced by Impact of Kinetic Energy Penetrator on a Steel Target," BRL Memorandum Report ARBRL-MR-02983, January 1980 (ADB 045141L).*

[2] *N. J. Huffington and S. R. Robertson, "Containment Structures Versus Suppressive Structures," BRL Memorandum Report BRL-MR-2587, February 1976 (ADA 021973).*

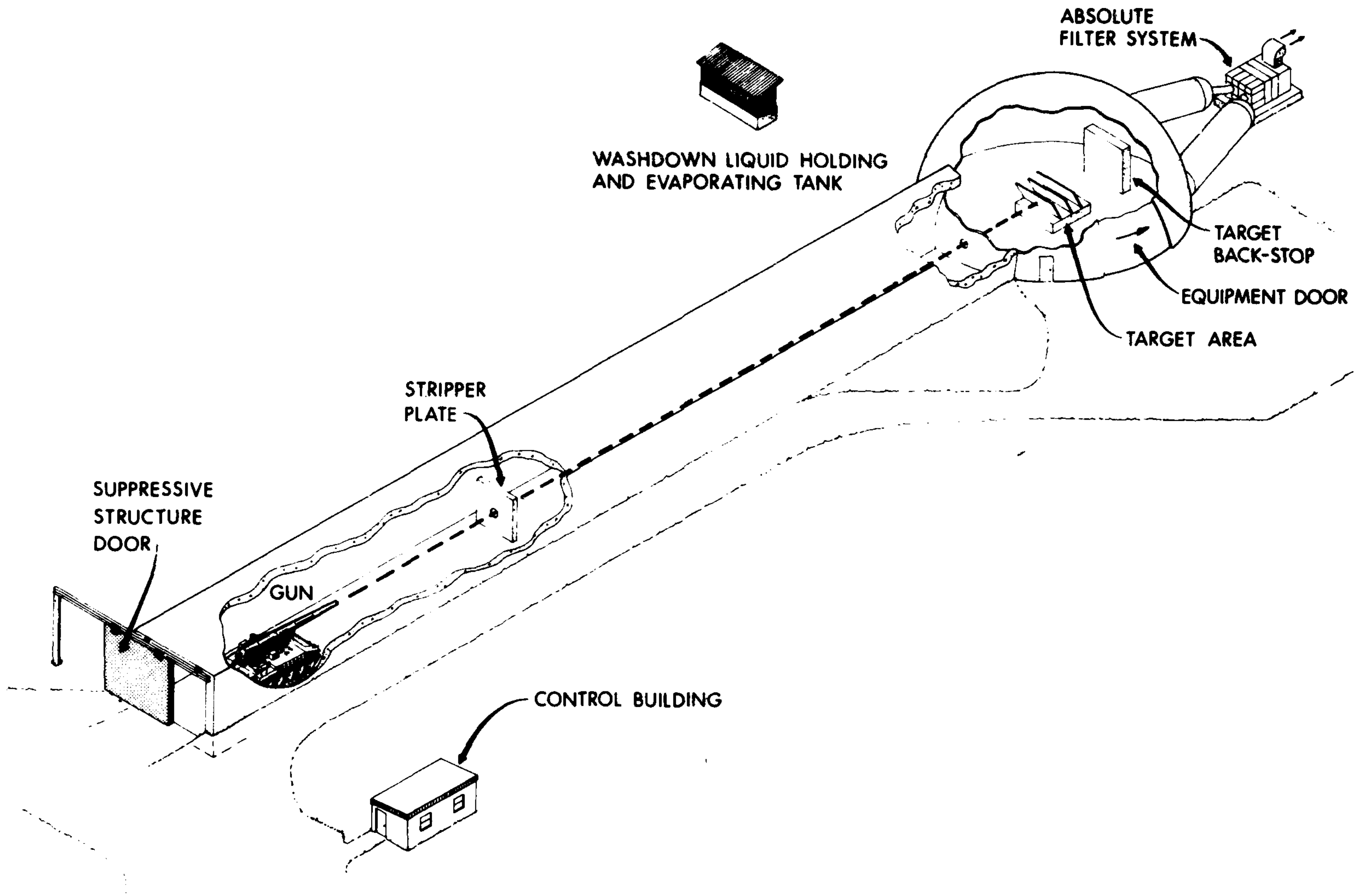

Figure 1. Preliminary Concept Layout of the AHKELS (Advanced High Kinetic Energy Launch System) Range.

subsequent objective was to perform an approximate conservative static analysis for an initial estimate of wall thickness. Finally the dynamic, elasto-plastic, large deflection response of the shell configuration clamped to a horizontal rigid foundation was studied to indicate critical locations where peak strains or deflections could occur.

II. ESTIMATION OF TRANSIENT LOADS

The transient loads were estimated under the assumption that the test firing of penetrator rounds would generate overpressures inside the containment chamber similar to those caused by an internal blast due to an equivalent central charge weight of 29.03 Kg* at the base as shown in Figure 2. Assuming the walls to be rigid, the symmetry of the charge and the structure about a vertical axis through the center indicates uniform distribution of internal reflected loading upon the structure. For the estimation of peak reflected overpressure, a conservative cube-root scaling law[3] is employed to compute the scaled distance, Z, of the wall from the charge location in the form

$$Z = \frac{R}{W_E^{1/3}} \qquad (1)$$

where W_E is the equivalent charge weight and R is the distance of the wall from the charge location.

Once the scaled distance is known the reflected parameters such as peak overpressure, impulse, time of arrival and duration time of the shock loading could be estimated from compiled air blast tables.[4,5] The decay of the reflected overpressure is assumed to obey the modified Friedlander exponential decay equation which can be written as

$$P_r = P_m[1 - t/t_o]e^{-\alpha t/t_o} \qquad (2)$$

where t_o is the positive phase duration of the impulse, P_m is the peak reflected overpressure and t is the elapsed time from arrival of blast wave at inner surface of the hemisphere. The exponential decay parameter, α, is calculated from

---

As per equivalent charge data provided by L. Giglio-Tos, Armor Mechanics Branch, Terminal Ballistics Division, BRL, September 1980.

[3] *Engineering Design Handbook, "Explosions in Air, Part One," AMC Pamphlet AMCP 706-181, Headquarters, US Army Materiel Command, pp. 3-5, July 1974.*

[4] *B. Soroka, "Air Blast Tables for Spherical 50/50 Pentolite Charges at Side-On and Normal Incidence," BRL Memorandum Report ARBRL-MR-02975, December 1979 (ADA 080537).*

[5] *H. Goodman, "Compiled Free Air Blast Data on Bare Spherical Pentolite," BRL Report BRL-R-1092, February 1960 (ADA 235278).*

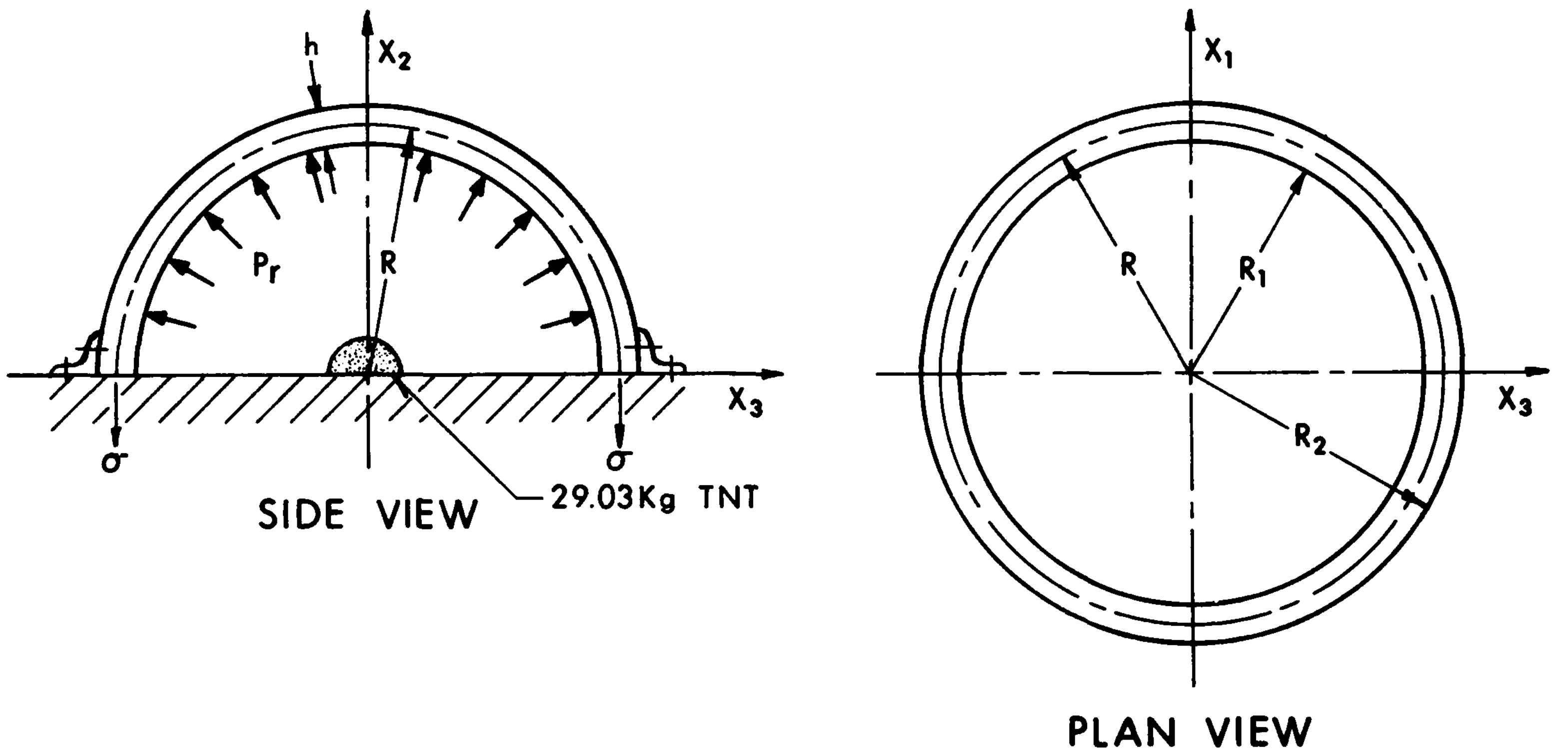

Figure 2. Sectional View Through the Hemispherical Containment Structure.

$$I_r = \frac{P_r t_o}{\alpha^2} (e^{-\alpha} + \alpha - 1) \tag{3}$$

where I_r is the reflected impulse. Values of P_r, I_r, and t_o were taken from tables listed in Reference 4. When α is determined, the complete reflected pressure versus time loading on the structure can be predicted.

III. ESTIMATION OF QUASI-STATIC LOADS

Quasi-static pressures immediately following the reflected pressure were predicted assuming that the heat of combustion of TNT is used totally to heat the air within the enclosure.[6] A relationship for the resultant increase in pressure is

$$\Delta P = \frac{0.4\, h_c W_E}{V}, \text{ kPa,} \tag{4}$$

where

$V = 1513.9\ m^3$, the internal volume of the enclosure,

$W_E = 29.03$ Kg, weight of the explosive charge, and

$h_c = 13.5$ kJ/g, the heat of combustion of TNT.

An internally pressurized structure vents the pressure to the surroundings through openings in its walls, causing a slow decay to ambient conditions as shown by Kinney and Sewell[7] and is computed from

$$\text{Ln } P = \text{Ln } P_o - .315\ (A_v/V)\ t_s, \tag{5}$$

where

t_s = elapsed time in ms

P = absolute pressure at t_s

$A_v = 2.33\ m^2$, the available vent area.

---

[6] *Edward M. Weyer, Editor-in-chief, Annals of the New York Academy of Sciences, Vol. 152, "Prevention of and Protection Against Accidental Explosion of Munitions, Fuels and other Hazardous Mixtures," Published by the Academy, 2 East Sixty-Third Street, New York, NY 10021, p. 317.*

[7] *G. F. Kinney and R. G. S. Sewell, "Venting of Explosives," NWC Technical Memorandum No. 2448, July 1974.*

The long-term duration of the decay is essentially due to the relatively small vent area available, causing a slow pressure decay to the atmosphere.

The blow-down time, t_g, required to reduce the residual overpressure to ambient conditions developed by Keenan et al,[8] based on the firing of high explosives in chambers with known vent areas and volumes, is given as

$$t_g = 6.28\ (A_v/V)^{-.86} \tag{6}$$

The above equation is valid for $A_v/V^{2/3} < 0.21$. In the current design the ratio, $A_v/V^{2/3}$, equals .018, and the duration time for the quasi-steady pressure is approximately 1600 ms.

The computation involves determination of peak residual overpressure from Equation (4) which when combined with Equations (5) and (6) yields the quasi-steady part of the loading history. The junction between the reflected overpressure history and the quasi-steady loading was smoothed by a curve interpolation scheme in order to avoid a sharp transition. The resulting load profile is shown in Figure 3. This loading is applied uniformly at each mesh point on the inside wall in the radial direction in the finite-difference structural response model in the PETROS 3.5 computer program[9] developed for the BRL. In Figure 3 the load-time history inside the hemispherical enclosure was zeroed out after 180 ms to facilitate damping of small elastic oscillations and to observe any residual deformation of the hemispheric wall. The peak reflected overpressure was found to be 257.3 kPa, while the peak residual overpressure was approximately 100 kPa.

IV. STATIC STRESS ANALYSIS

Prior to a detailed dynamic response study, a static stress analysis in the linear-elastic-small deflection regime was conducted to obtain an initial estimate of the enclosure wall thickness. In this investigation discontinuity stresses at the base of the shell structure were ignored. Since the duration of the reflected pressure is less than 1.5 ms compared to 1600 ms for the duration of the quasi-steady overpressure, an approximate static analysis based on a minimum factor of safety of 2.0 is considered to be satisfactory. For the preliminary investigation, stress-concentration near holes, cutouts and wall openings was neglected. However, the effect of ground-plane reflection

---

[8] *W. A. Keenan and J. A. Tamareto, "Blast Environment from Fully and Partially Vented Explosions in Cubicles," U.S. Naval Civil Engineering Laboratory Technical Report No. 51-027, February 1974.*

[9] *S. D. Pirotin, B. A. Berg and E. A. Witmer, "PETROS 3.5: New Developments and Program Manual for the Finite-Difference Calculation of Large Elastic-Plastic Transient Deformations of Multi-Layer Variable-Thickness Shells," U.S. Army Ballistic Research Laboratories Contract Report No. 211, February 1975 (ADA 007215).*

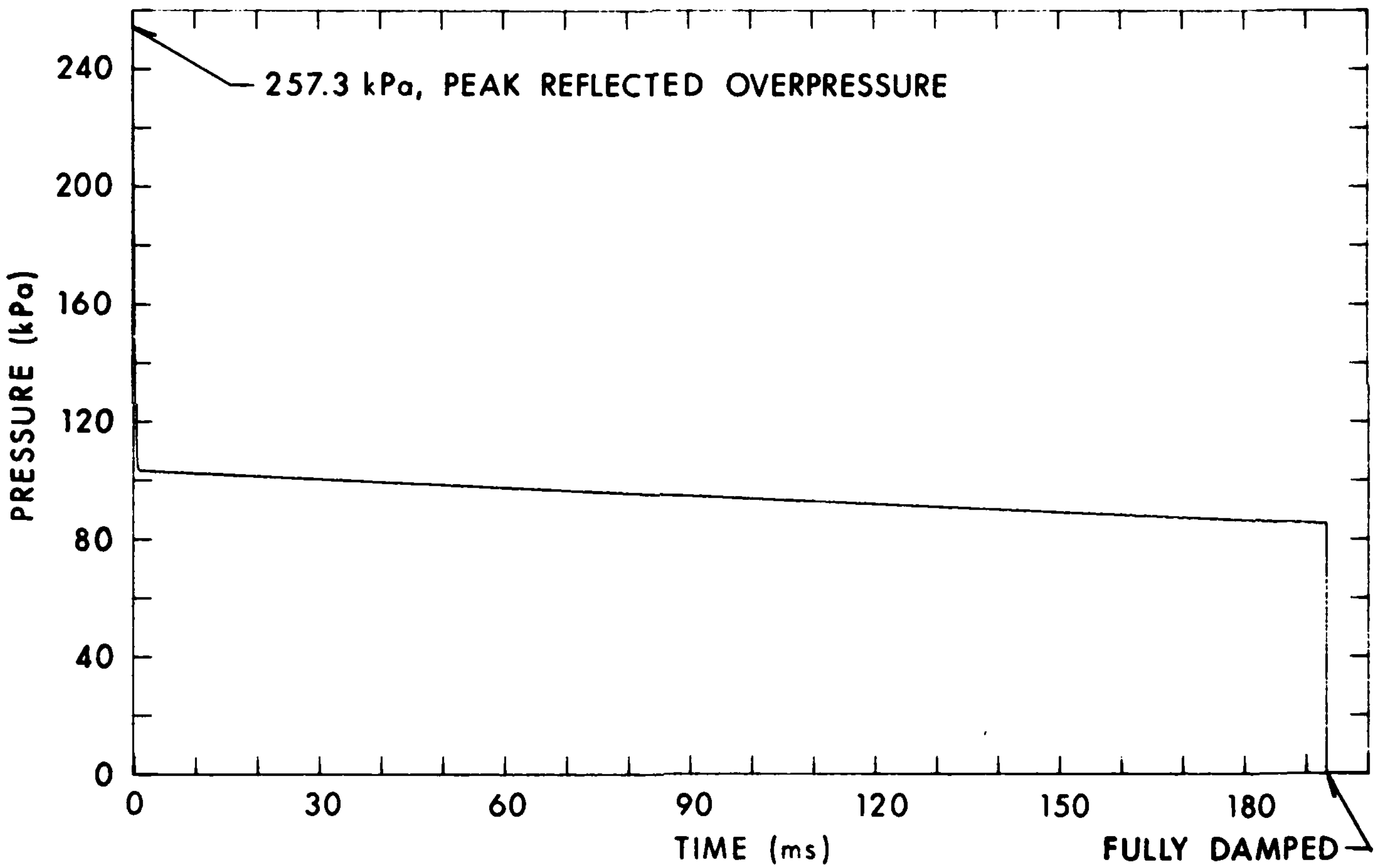

Figure 3. Computed Pressure-Time History Due to Internal Explosive Blast Loading of the Hemispherical Enclosure.

of the shock wave was included through a load multiplication factor of $k = 2.0$, which in effect doubled the applied load.

To contain the initial pressure pulse in an elastic manner, only the peak reflected overpressure, P_m, was included in the calculation of stresses and deflections. An equivalent static meridional stress, σ, can be calculated from Figure 2 by equating the resultant upward force due to internal pressurization to the net downward restraining force due to the stress developed at the clamped edge, resulting in

$$\sigma = \frac{RkP_m}{2h} \tag{7}$$

where

$R = 8.987$ m, the median radius

k = load multiplication factor

However, for an assumed factor of safety of 2.0, $\sigma = \frac{1}{2}\sigma_y$, where σ_y is the static yield stress. Substituting this value of σ in Equation (7) and rearranging terms results in an expression for the estimated thickness, h, in the form

$$h = \frac{RkP_m}{\sigma_y} \tag{8}$$

The yield stress, σ_y, for the wall material which is 1020 steel is 241.3 MPa. Hence the wall thickness, h, from Equation (8) is found to be 19 mm.

Up to this point no consideration has been given to the possibility that fragment-induced damage to a shell might result in catastrophic rupture when the blast loading is applied. One should estimate the material removal produced by the impact of the worst threat fragment and perform a local three-dimensional analysis of the stress field to determine whether a crack would be propagated under such loading. This problem in fracture mechanics is difficult to analyze and can be at least partially circumvented by a conservative selection of wall thickness under the assumption that the residual thickness is capable of withstanding the peak quasi-steady pressure even when a 50% depth of penetration has been achieved by a part-through fragment. The final thickness chosen was 25.4 mm (1 in), a material thickness which is readily available. The 25.4 mm thickness corresponds to a stress level of 45.5 MPa which when compared to the yield stress results in a final margin of safety of 4.3 which is satisfactory.

The peak radial deflection ΔR at the pole is estimated from Reference 10 as

[10] *R. J. Roark, "Formulas for Stress and Strain," Fifth Edition, McGraw-Hill Book Company, New York, NY, pp. 96, 451, 1975.*

$$\Delta R = \frac{R^2 k P_r (1-\nu)}{2Eh} \qquad (9)$$

where E, ν are elastic material properties.

The peak radial elastic deflection at the pole from Equation (9) was 1.1 mm, which is quite small and is consistent with the design objective. The gross mass of the hemispherical enclosure was approximately 96400 kg based on a 25.4 mm wall thickness. In this study allowance was made for the weight of flanged material at the base but not for extra weight associated with access provisions, welds or foundations.

To detect resonance due to coupling of the duration time of the pressure pulse with the natural vibration period, the time period, T, was calculated from Reference 10 as

$$T = \pi R \sqrt{\frac{2\rho(1-\nu)}{E}}\ , \qquad (10)$$

where ρ is the mass density. Further check of interaction of the reflected pressure pulse due to ground plane reflection with the elastic oscillation of the pole did not reveal any significant problem.

V. OPTIMIZATION STUDY

An optimization study based on equivalent strength showed substantial weight saving for a hemispherical configuration at or below 6 m radius but marginal savings at higher radius up to 9 m due to compensating thickness increases. An equation proposed by R. Karpp et al [11] for the minimum amount of vessel material V_m to contain a specified charge is given as

$$V_m = 4\pi W_E \left(\frac{K}{\epsilon_Y}\right)^{1.0406} \rho^{.0406} \left(\frac{R}{h}\right)^{.0406} \qquad (11)$$

where ϵ_Y is the yield point strain of the vessel material in biaxial tension, W_E is the charge weight, ρ is the density of the vessel material and K is an empirical curve-fit constant found to be 4.08×10^{-6} m^3/kg. Although the minimum amount of vessel material to contain a specific charge is not the governing design criterion, there may be some interest in determining the optimized value. If the volume of vessel material is plotted as a function of the radius-to-thickness ratio of the container as given in Equation (11), a slow variation is observed in the amount of vessel material required to contain the dynamic load as a function of the radius-to-thickness ratio R/h. The variation in material volume over the design range of $350 < R/h < 200$ is only

[11] *R. R. Karpp, T. A. Duffey and T. R. Neal, "Response of Containment Vessels to Explosive Blast Loading," Report No. LA-8082, UC 38, Los Alamos Scientific Laboratory, Los Alamos, New Mexico, June 1980.*

about 3%. Thus, the amount of material required to contain a specified charge in this range of configurations is essentially constant. Very thin wall, large-radius vessels with $R/h > 400$ make inefficient use of material, at least for blast wave containment. On the other hand, for thick wall, small-radius vessels with $R/h < 150$, at least 12% or higher saving in material volume can be realized with judicious choice of reinforcement in critical sections. Unfortunately, substantial saving in material could not be achieved due to constraints of minimum work space and equipment access considerations and the additional requirement of part-through fragment containment with 50% depth of penetration.

The analysis so far applies only to the containment of the initial pressure pulse. However, for long-term containment the volume of vessel material V required to contain the static pressure elastically can be estimated from the semiempirical relationship given in Reference 11 as

$$V_s = C \frac{W_E}{P_o} \tag{12}$$

where C is a constant with a value of about 1.3 m^3 MPa/kg for most solid explosives and P_o is the peak static pressure. The material volume appears to be independent of the radius-to-thickness ratio if the internal radius is approximated by the average radius of the vessel and the usual formula for equilibrium of a thin shell is used. Based on Equation (12) the material volume required to contain the static load was found to be approximately 20% of that required to contain the initial dynamic load.

A comparison of the 9 m hemispherical structure with an equivalent 9 m × 9 m × 7.3 m rectangular parallelepiped all welded depleted uranium (DU) containment structure[12] with a .07 m thick steel armor wall liner and a .064 m thick roof liner indicated an increase of 64 times in containment capacity of equivalent charge weight for the hemispherical structure with a 50% reduction in weight and concurrent doubling of the internal volume capacity without any significant sacrifice in the minimum margin of safety. In addition the simplistic design of the hemispherical enclosure, although somewhat difficult to fabricate, was a significant improvement for static and dynamic load bearing considerations. The down time for duration of residual overpressure was decreased substantially due to availability of larger entrance hole diameter and vent area from 3.33 sec total venting time at the R-14 range to approximately 1.5 sec at the R-9 firing range.

VI. DYNAMIC RESPONSE ANALYSIS

Response of the structure subjected to transient loads from an internal blast shown in Figure 2 was conducted using the BRL version of the PETROS 3.5 computer program [9], which employs the finite-difference method to solve the

[12] *A. D. Gupta, "Stress Analysis of the Target Enclosure of the R-14 Firing Range," Unpublished Report, BRL, 1980.*

nonlinear equations governing finite-amplitude elastoplastic response of thin Kirchhoff shells. The model is valid for large deflections and can be employed to treat the entire structure rather than a small section.

A. Material Model

The uniaxial tensile quasi-static stress-strain property for 1020 steel which is used as the primary vessel material is shown by the continuous line in Figure 4. The material is modeled in the code as a combination of three linear segments indicated as the dashed curve in Figure 4 followed by a perfectly plastic behavior and linear elastic-plastic unloading, resulting in a polygonal approximation of the experimental data. The strain-hardening part of the stress-strain curve is generated by a sublayer hardening model from a weighted combination of elastic perfectly-plastic curves, yielding a piecewise multilinear hardening representation. Strain-rate effects were neglected, which is conservative since these effects increase the structural resistance and thus reduce the total deformation.

B. Finite-Difference Model

Since both the responding structure and the applied loads are symmetric with respect to the vertical axis as shown earlier in Figure 2, it is sufficient to model the response of a single pie-shaped segment of the hemispherical enclosure and generate the entire structure by 360° rotation of the structure about the axis of symmetry, resulting in quite economical computer runs.*

A total of 18 meshes along the surface and a single layer through the thickness were used to represent the pie-shaped segment. Four Gaussian integration points through the thickness were used at each mesh for computational purpose. Total number of mesh points did not exceed 37. Initial configuration of the finite-difference model employed for all subsequent calculations is shown in Figure 5.

VII. RESULTS AND DISCUSSION

The deformed cross section of the hemispherical segment at 36 ms relative to the initial undeformed configuration is shown in Figure 6. At this time the maximum deflection occurs at the pole. The deflections are exaggerated due to a high magnification factor of 1000 and are, in fact, small enough to be in the linear elastic range, in accordance with the design objective.

Figure 7 describes the transient rectangular components of displacement in a meridional plane at point A at 45° from the vertical axis of the hemisphere. The maximum displacement at this point is only 1.028 mm, essentially radially outward. Displacements at other locations are correspondingly small except in the neighborhood of the pole of the hemisphere where a peak deflection of 1.17 mm is observed at approximately 36 ms as illustrated in Figure 8. However, this displacement is less than 4% of the shell thickness so that

**Since design parameters for the entrance hole, exhaust openings and the equipment access door were not finalized in the preliminary concept, a continuous configuration was considered for this investigation.*

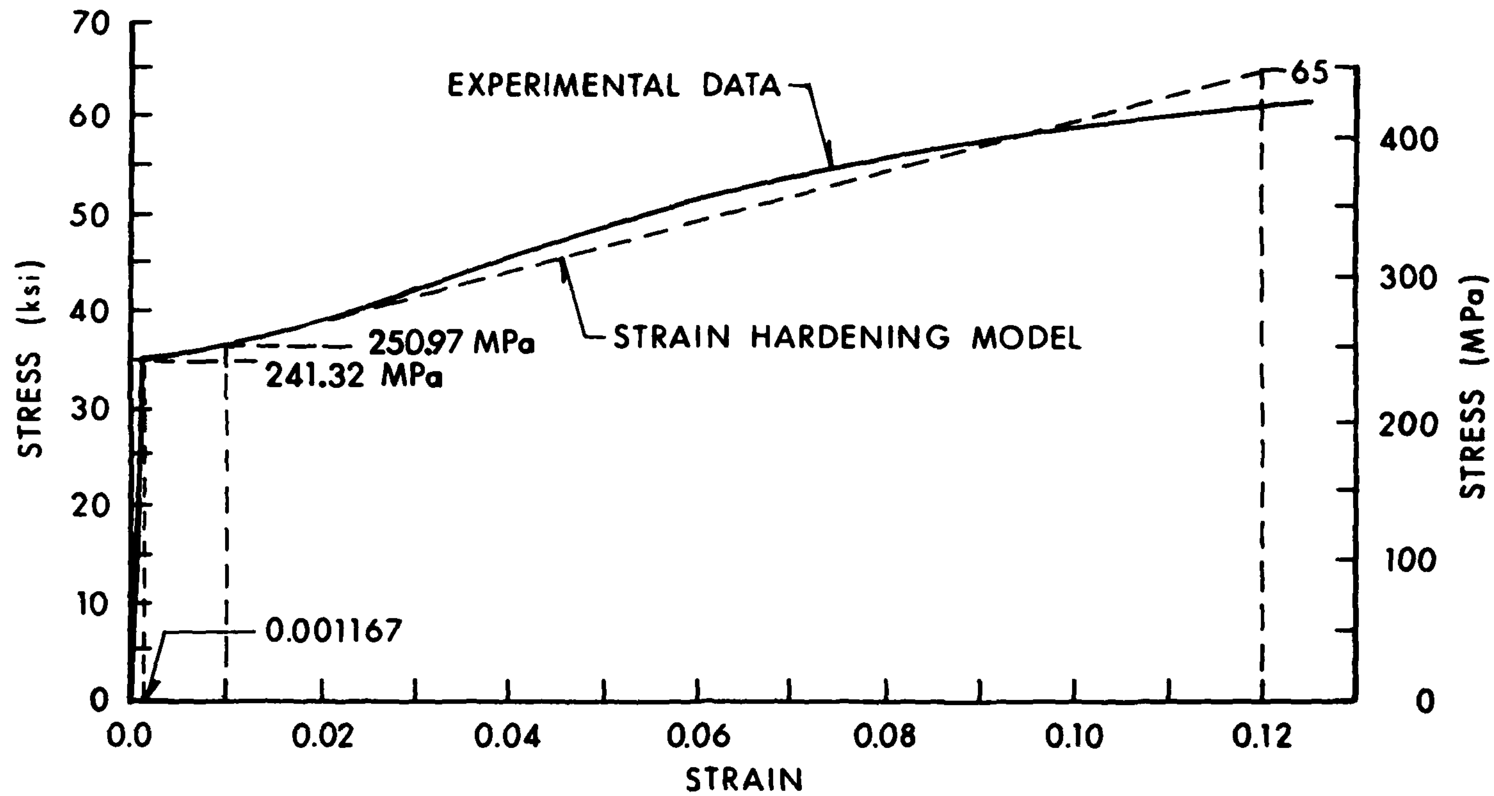

Figure 4. Stress-Strain Property Modeling.

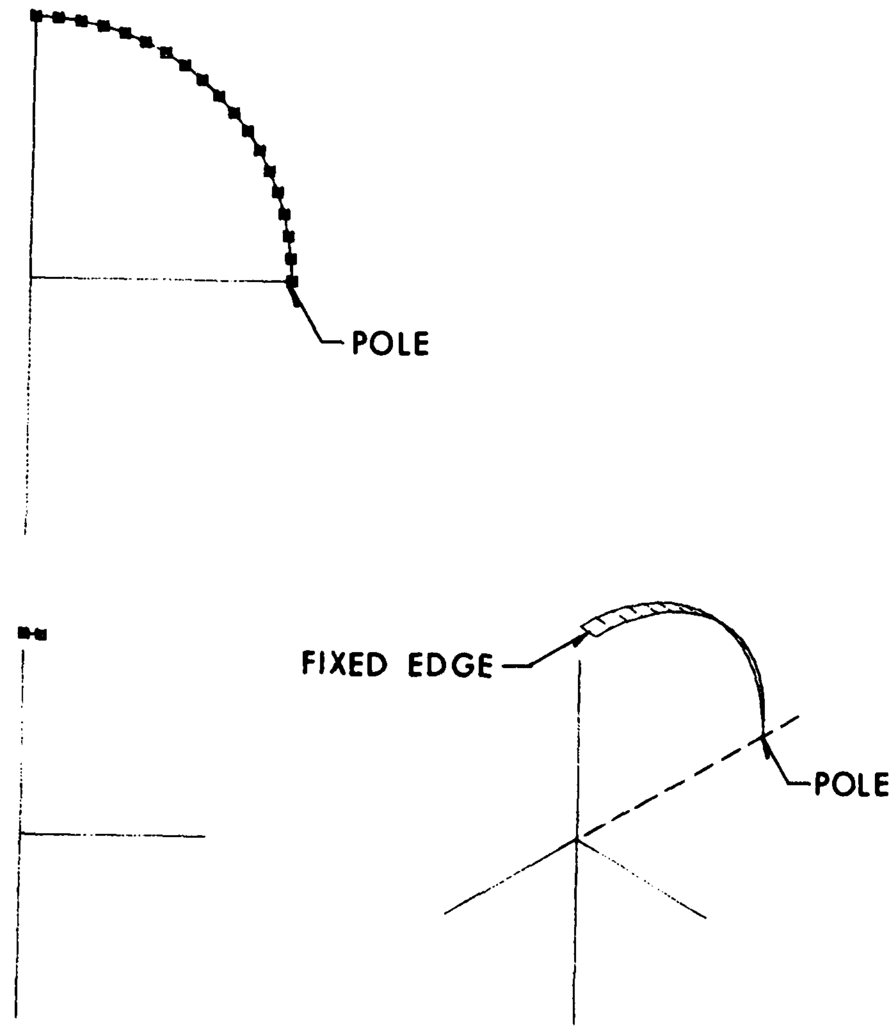

Figure 5. Initial Configuration of the Finite-Difference Model.

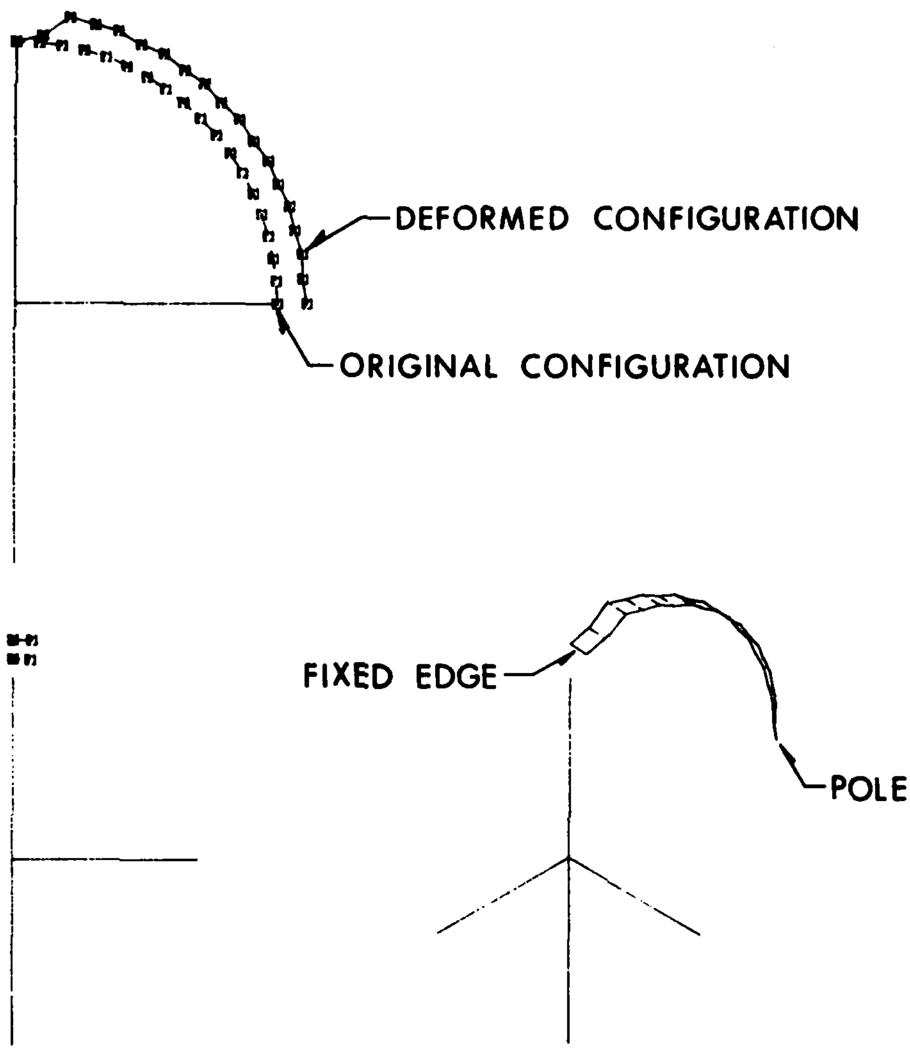

Figure 6. Deformed Configuration at 36 ms Corresponding to Cycle No. 1500.

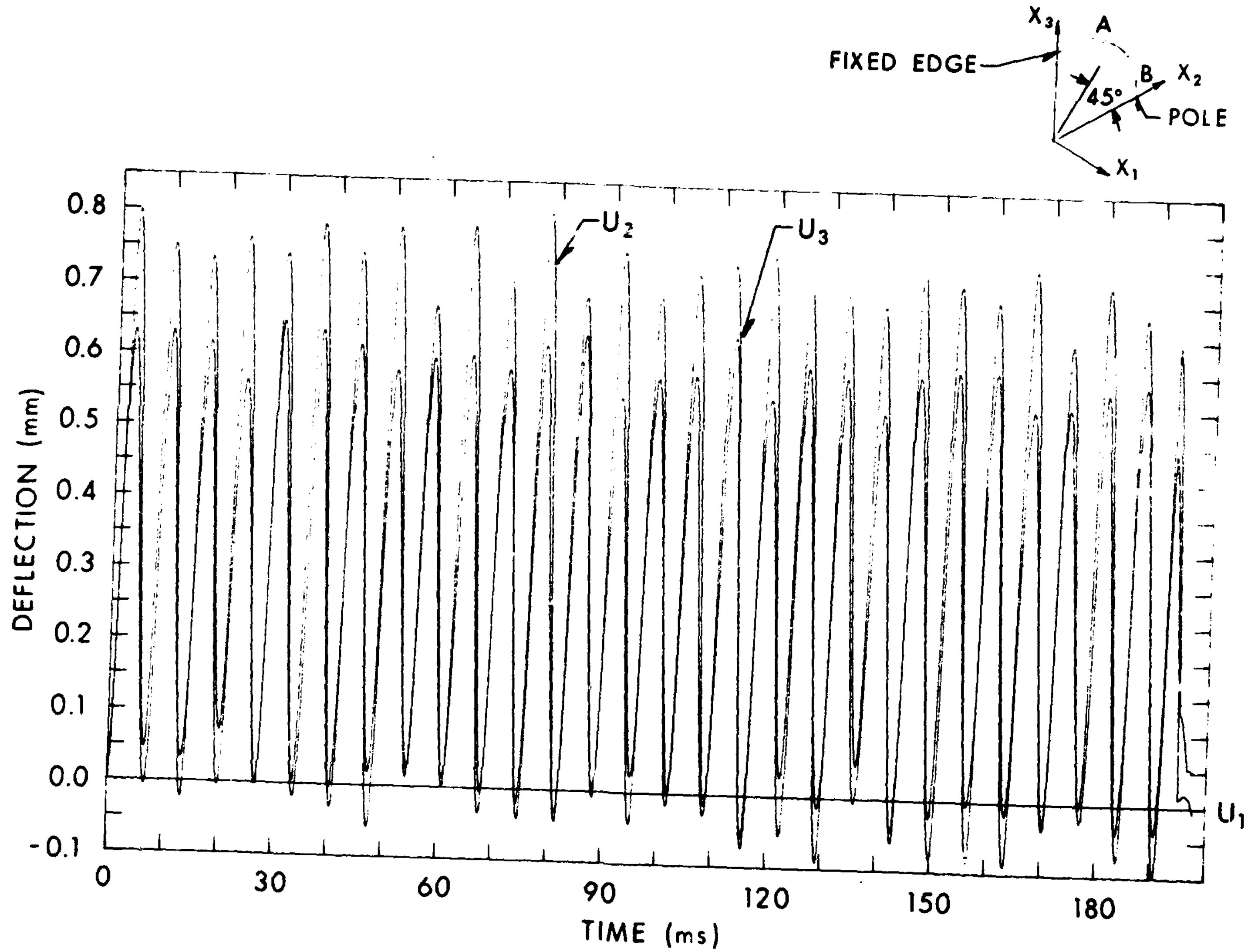

Figure 7. Transient Displacement Components at Point A.

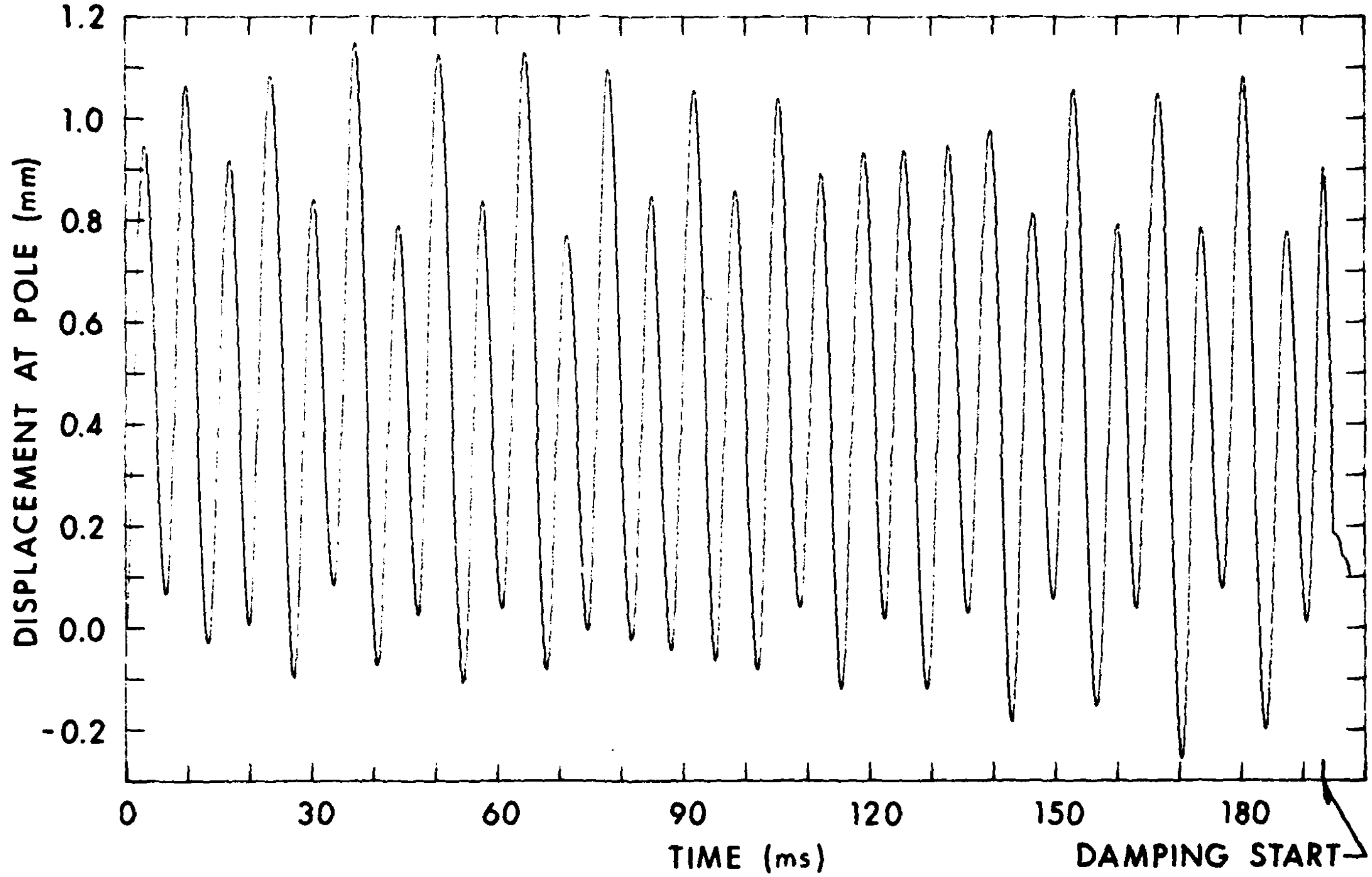

Figure 8. Transient Displacement at the Pole of the Hemisphere.

geometric nonlinearities are insignificant. The larger response at the pole is attributed to focusing of flexural vibratory energy.[2]

The PETROS 3.5 code was run for 8000 cycles (192 ms) in an undamped mode, after which artificial damping was introduced to suppress the elastic oscillations which were positively biased due to residual internal pressure. Damping was facilitated by zeroing out the internal pressure. The fully damped condition was achieved at cycle 8235 (198 ms) when the final configuration was found to be identical to the undeformed configuration in Figure 5 with no evidence of permanent plastic deformation.

Energy balance studies using the code confirmed absence of plastic work and numerical instability. Both total and kinetic energies were bounded. The fluctuations of kinetic energy appeared to have twice the frequency of the work performed by the internal blast pressure.

Transient strain components on the outer and inner surfaces of the hemisphere at a point near the edge are shown in Figures 9a and 9b, respectively. The meridional strain components on the inner and outer surfaces are almost in phase initially but become out of phase and unequal in magnitude with increasing time signaling the buildup of some flexural deformation. The hemisphere moves outward and inward, except at the fixed boundary, in a spherically symmetric breathing mode resulting in membrane strains upon which the bending strains are subsequently superposed due to propagation of flexural waves from the fixed boundary towards the pole. Significant difference in strains between the outer and the inner walls at the clamped edge could be primarily attributed to domination of the response by the bending strains. The circumferential strains indicated by continuous lines in Figures 9a and 9b are zero as expected. Calculations for maximum meridional stress based on peak strain results in a stress level of 48.26 MPa, which is equivalent to a safety margin of 4.0. As expected from elastic theory, peak strains occurred at the fixed edge, while maximum deflection occurred at the pole.

The variation of strain at the inner wall with time at a point near the pole is shown in Figure 10. The continuous line depicts the circumferential strain, which is in phase and very similar to the meridional strain shown by the intermittent line. The strains at the outer wall near the pole exhibit elastic oscillations of approximately the same magnitude and duration as in Figure 10. This behavior indicates substantial weakening of the flexural wave near the pole and domination of meridional and circumferential strains by the membrane component of strain due to elastic vibration of the wall in the breathing mode. The peak meridional stress at the pole was calculated based on elastic equations and was found to be approximately 25 MPa, which is considerably lower than the maximum stress at the clamped edge. The stress level is equivalent to a safety margin of 8.6 based on the yield stress.

Both strain components are relieved completely upon damping at approximately 198 ms. An isometric view of the fully damped configuration generated by 360° rotation of the pie-shaped segment about the axis of symmetry is shown in Figure 11. The view through Section A-A in this figure depicts the final configuration upon damping superposed on the initial configuration. The coincidence of the two configurations at a high magnification ratio of 1000 indicates the absence of any plastic deformation and confirms small strains and deformations throughout the structure in accordance with earlier results.

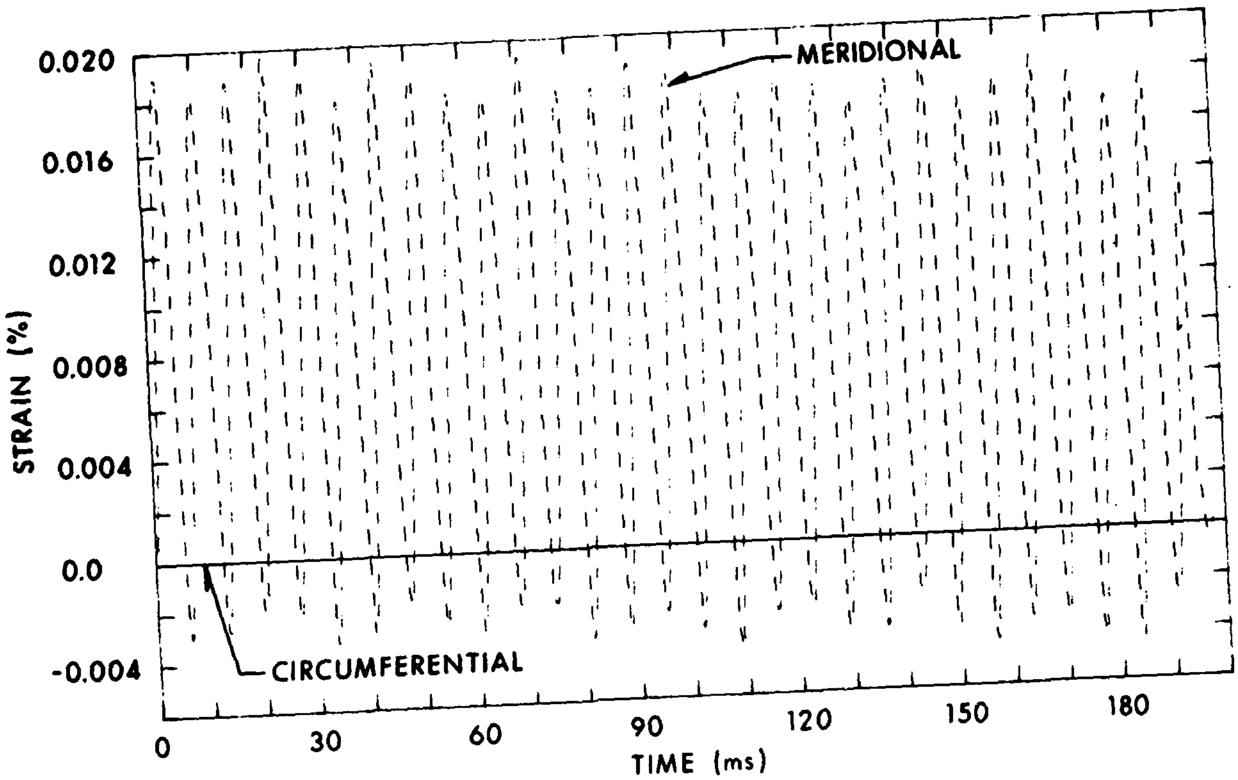

(a) Outer Surface Strain Components.

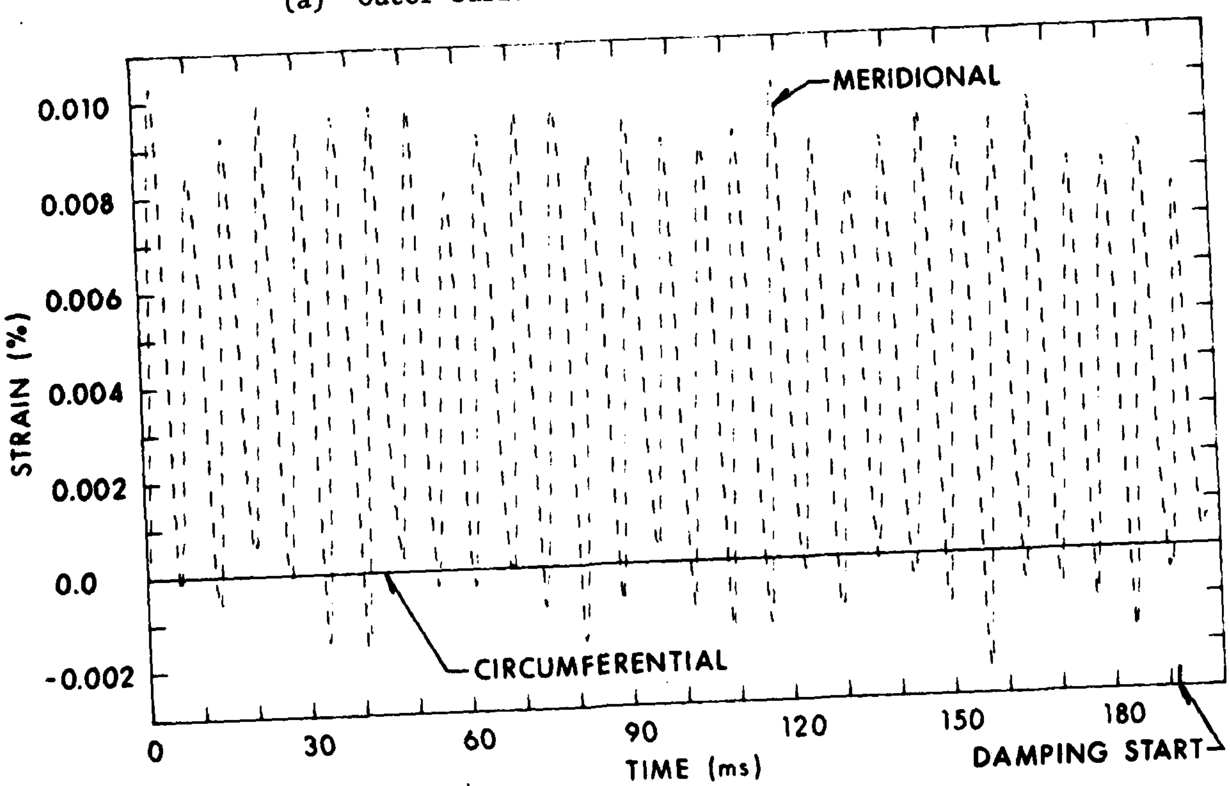

(b) Inner Surface Strain Components.

Figure 9. Surface Strains at the Fixed Edge.

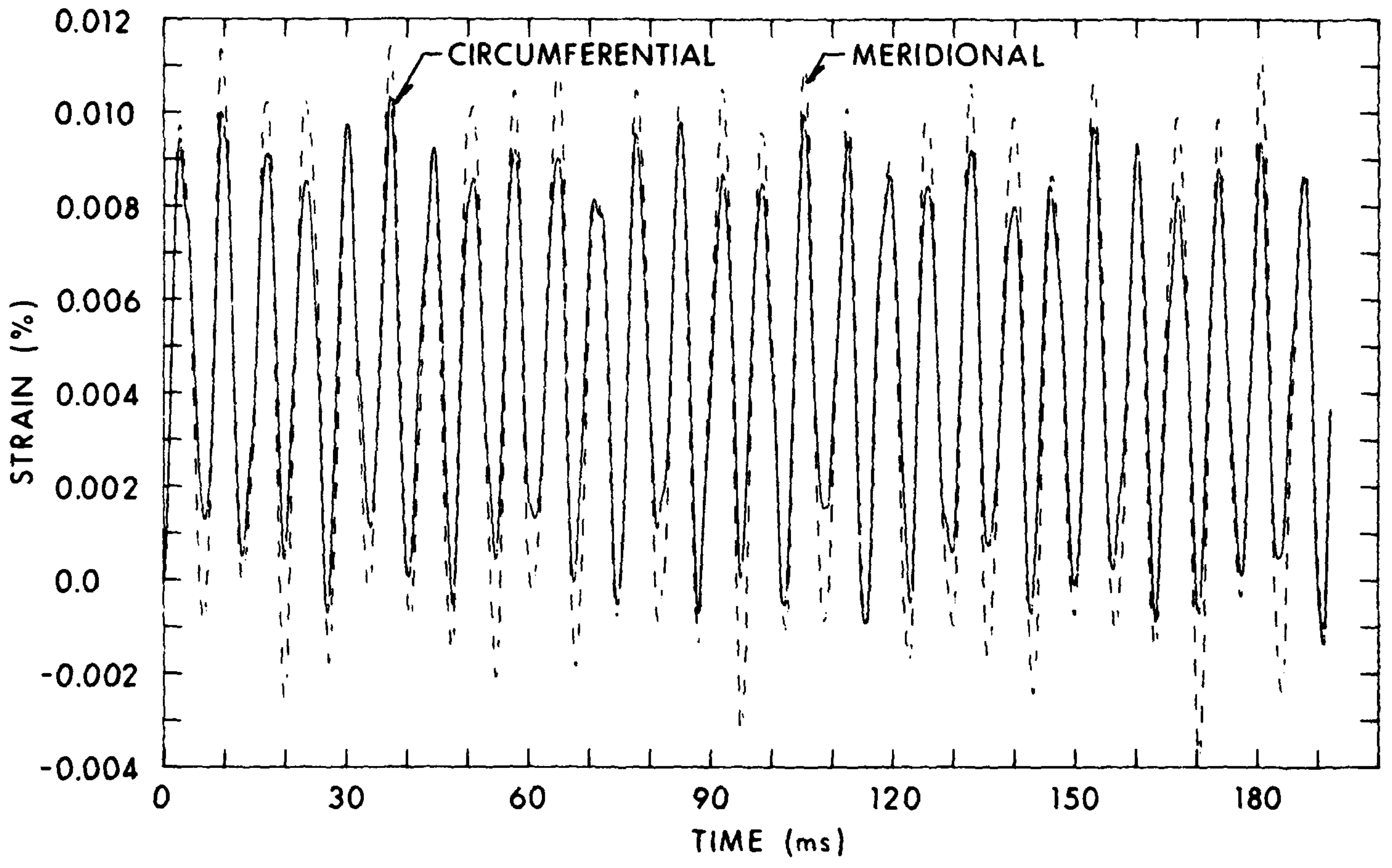

Figure 10. Surface Strains at the Inner Wall Near the Pole.

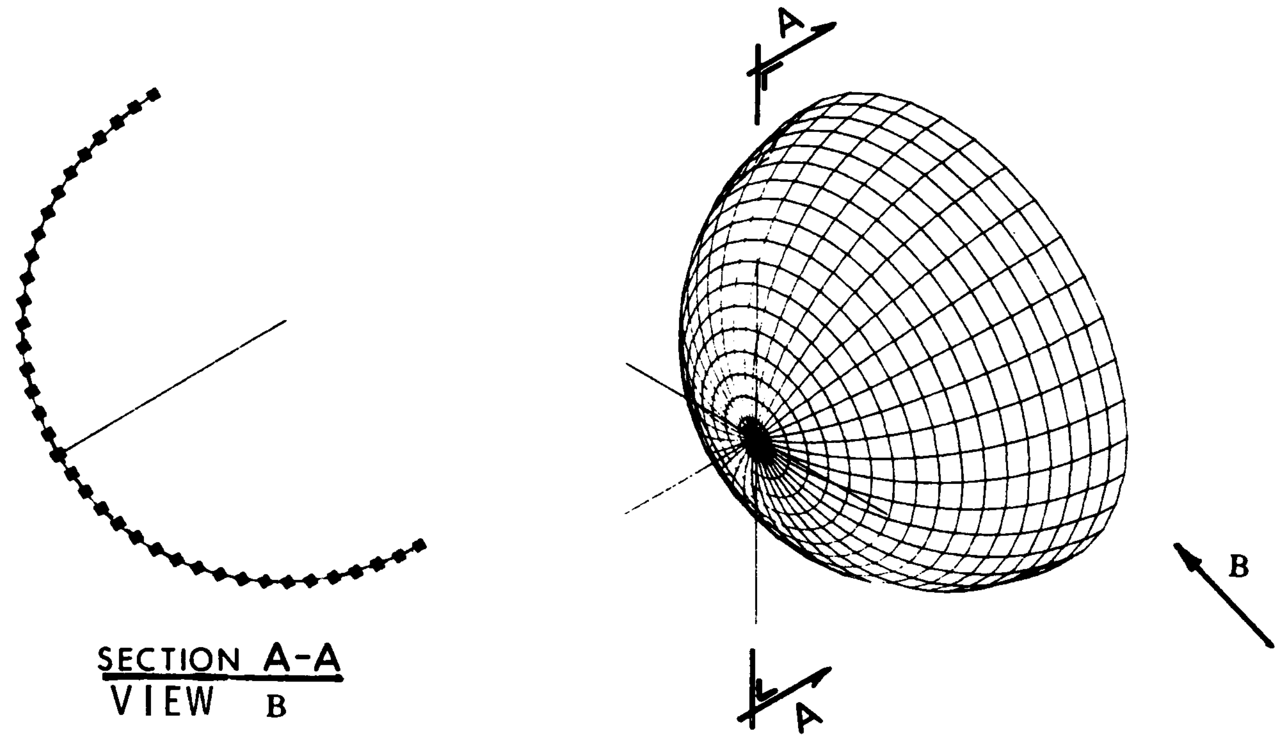

Figure 11. Isometric and Sectional View of the Fully Damped Configuration.

VIII. CONCLUDING REMARKS

It has been demonstrated, through use of a rigorous nonlinear shell response methodology, that it is possible to design a containment structure with a hemispherical configuration in an efficient and cost effective manner. The methodology could be easily extended to structural optimization studies, resulting in considerable cost savings provided internal volume and access considerations could be met.

In spite of simplifying assumptions and limitations of the PETROS 3.5 version of the shell response analysis code which neglects transverse shear deformation and rotatory inertia, the analysis gives a clear insight into the initial loading mechanism due to structural resistance and interaction of various components of the response. However, an examination of the characteristics of the hemispherical structure reveals the following:

1. The 9 m radius, .0254 m thick hemispherical enclosure is an efficient protective structure capable of withstanding internal blast from a 29.03 kg TNT charge with assured structural integrity.

2. The structure is capable of successful containment of combustion products and fragments with sufficient mass and velocity to achieve a 50% depth of penetration with a satisfactory margin of safety.

3. Peak deflection occurs at the pole due to elastic oscillations of the structure in the breathing mode resulting from focusing of vibratory energy at the pole.

4. Peak strain occurs at the clamped edge and exhibits considerable difference in strain magnitude between the inner and outer surfaces due to bending waves originating in this region.

5. The ratio of the vent area to the internal volume is small enough to result in a slow rate of venting and an extended venting time of 1600 ms for the quasi-steady residual overpressure to blow down to the external ambient conditions.

6. Cumulative damage effect due to repeated test firings could conceivably cause low cycle fatigue of the structure, and a periodic inspection of the internal surface and joints for cracks in critical regions is recommended.

7. Future work should be directed to modelling of the enclosure structure with wall openings for the equipment and personnel access doors, protective walls for X-ray equipments, detailed analysis of critical joints and stress concentration due to holes and cutouts in corner regions.

ACKNOWLEDGEMENTS

This investigation was performed for Mr. Louis Giglio-Tos, who was the Project Coordinator for Project No. T01400 at R-9. Valuable assistance of Mr. Charles N. Kingery, Dr. Joseph M. Santiago and Mr. Frederick H. Gregory of the Terminal Ballistics Division is gratefully acknowledged.

REFERENCES

1. R. Abrahams, R. Peterson, and B. Bertrand, "Measurement of Blast Pressure Produced by Impact of Kinetic Energy Penetrator on a Steel Target," BRL Memorandum Report ARBRL-MR-02983, January 1980 (ADB 045141L).

2. N. J. Huffington and S. R. Robertson, "Containment Structures Versus Suppressive Structures," BRL Memorandum Report BRL-MR-2597, February 1976 (ADA 021973).

3. Engineering Design Handbook, "Explosions in Air, Part One," AMC Pamphlet AMCP 706-181, Headquarters, U.S. Army Materiel Command, pp. 3-5, July 1974.

4. B. Soroka, "Air Blast Tables for Spherical 50/50 Pentolite Charges at Side-On and Normal Incidence," BRL Memorandum Report ARBRL-MR-02975, December 1979 (ADA 080537).

5. H. Goodman, "Compiled Free Air Blast Data on Bare Spherical Pentolite," BRL Report BRL-R-1092, February 1960 (ADA 235278).

6. Edward M. Weyer, Editor-in-chief, Annals of the New York Academy of Sciences, Vol. 152, "Prevention of and Protection Against Accidental Explosion of Munitions, Fuels and other Hazardous Mixtures," Published by the Academy, 2 East Sixty-Third Street, New York, NY 10021, p. 317.

7. G. F. Kinney and R. G. S. Sewell, "Venting of Explosives," NWC Technical Memorandum No. 2448, July 1974.

8. W. A. Keenan and J. A. Tamareto, "Blast Environment from Fully and Partially Vented Explosions in Cubicles," U.S. Naval Civil Engineering Laboratory Technical Report No. 51-027, February 1974.

9. S. D. Pirotin, B. A. Berg and E. A. Witmer, "PETROS 3.5: New Developments and Program Manual for the Finite-Difference Calculation of Large Elastic-Plastic Transient Deformations of Multi-Layer Variable-Thickness Shells," U.S. Army Ballistic Research Laboratories Contract Report No. 211, February 1975 (ADA 007215).

10. R. J. Roark, "Formulas for Stress and Strain," Fifth Edition, McGraw-Hill Book Company, New York, NY, pp. 96, 451, 1975.

11. R. R. Karpp, T. A. Duffey and T. R. Neal, "Response of Containment Vessels to Explosive Blast Loading," Report No. LA-8082, UC 38, Los Alamos Scientific Laboratory, Los Alamos, New Mexico, June 1980.

12. A. D. Gupta, "Stress Analysis of the Target Enclosure of the R-14 Firing Range," Unpublished Report, BRL, 1980.

LIST OF SYMBOLS

α	exponential decay parameter
ε_Y	yield strain in biaxial tension
ν	Poisson's ratio
ρ	density of material, kg/m^3
σ	meridional stress, kPa
σ_y	static yield stress, kPa
A_v	available vent area, m^2
E	modulus of elasticity, MPa
K	empirical curve-fit constant = 4.08×10^{-6} m^3/kg
P_m	peak reflected overpressure, MPa
P_o	peak quasi-static pressure, MPa
P_r	reflected overpressure, MPa
R	mean radius of the hemisphere, m
ΔR	peak radial deflection at the pole, m
T	time period of oscillation, ms
V	internal enclosure volume, m^3
V_m	minimum volume of vessel material, m^3
V_s	volume of vessel material to contain static pressure, m^3
W_E	equivalent charge weight of explosive, kg
Z	scaled distance of the wall from the charge location, $m/kg^{1/3}$
h	wall thickness, m
t_g	blow-down time, ms
t_o	positive phase duration of impulse, ms
t_s	elapsed time from arrival of blast wave at inner surface of hemisphere, ms

DISTRIBUTION LIST

No. of Copies	Organization
12	Administrator Defense Technical Info Center ATTN: DTIC-DDA Cameron Station Alexandria, VA 22314
1	Director of Defense Research & Engineering ATTN: DD/TWP Washington, DC 20301
1	Asst. to the Secretary of Defense (Atomic Energy) ATTN: Document Control Washington, DC 20301
1	Director Defense Advanced Research Projects Agency ATTN: Tech Lib 1400 Wilson Boulevard Arlington, VA 22209
2	Director Federal Emergency Management Agency ATTN: Mr. George Sisson/RF-SR Technical Library Washington, DC 20301
1	Director Defense Intelligence Agency ATTN: DT-2/Wpns & Sys Div Washington, DC 20301
1	Director National Security Agency ATTN: E. F. Butala, R15 Ft. George G. Meade, MD 20755
1	Director Joint Strategic Target Planning Staff JCS Offut AFB Omaha, NB 68113
1	Director Defense Communications Agency ATTN: 930 Washington, DC 20305
5	Director Defense Nuclear Agency ATTN: STSI/Archives SPAS STSP STVL/Dr. La Vier RATN Washington, DC 20305
6	Director Defense Nuclear Agency ATTN: DDST/Dr. Conrad SSTL/Tech Lib (2 cys) SPSS/K. Goering G. Ullrich SPTD/T. Kennedy Washington, DC 20305
2	Commander Field Command, DNA ATTN: FCPR FCTMOF Kirtland AFB, NM 87115
1	Commander Field Command, DNA Livermore Branch ATTN: FCPRL P.O. Box 808 Livermore, CA 94550
1	Director Inst for Defense Analyses ATTN: Library 400 Army Navy Drive Arlington, VA 22202

DISTRIBUTION LIST

No. of Copies	Organization
1	Director US Army Air Mobility Research and Development Laboratory Ames Research Center Moffett Field, CA 94035
1	Commander US Army Communications Rsch and Development Command ATTN: DRDCO-PPA-SA Fort Monmouth, NJ 07703
3	Commander US Army Electronics Research and Development Command ATTN: DELSD-L DELEW-E, W. S. McAfee DELSD-EI, J. Roma Fort Monmouth, NJ 07703
8	Commander US Army Harry Diamond Labs ATTN: Mr. James Gaul Mr. L. Belliveau Mr. J. Meszaros Mr. J. Gwaltney Mr. F. W. Balicki Mr. Bill Vault Mr. R. J. Bostak Mr. R. K. Warner 2800 Powder Mill Road Adelphi, MD 20783
4	Commander US Army Harry Diamond Labs ATTN: DELHD-TA-L DRXDO-TI/002 DRXDO-NP DELHD-RBA/J. Rosado 2800 Powder Mill Road Adelphi, MD 20783
1	Commander US Army Missile Command ATTN: DRSMI-YDL Redstone Arsenal, AL 35898
1	Commander US Army Missile Command ATTN: DRSMI-R Redstone Arsenal, AL 35898
4	Commander US Army Natick Research and Development Command ATTN: DRDNA-DT, Dr. D. Sieling DRXNE-UE/A. Johnson A. Murphy W. Crenshaw Natick, MA 01762
1	Commander US Army Tank Automotive Rsch and Development Command ATTN: DRDTA-UL Warren, MI 48090
1	Commander US Army Foreign Science and Technology Center ATTN: Rsch & Concepts Br 220 7th Street, NE Charlottesville, VA 22901
1	Commander US Army Logistics Center ATTN: ATCL-O Mr. Robert Cameron Fort Lee, VA 23801
3	Commander US Army Materials and Mechanics Research Center ATTN: Technical Library DRXMR-ER, Joe Prifti Eugene de Luca Watertown, MA 02172

DISTRIBUTION LIST

No. of Copies	Organization
1	Program Manager US Army BMD Program Office ATTN: John Shea 5001 Eisenhower Avenue Alexandria, VA 22333
2	Director US Army BMD Advanced Technology Center ATTN: CRDABH-X CRDABH-S Huntsville, AL 35804
1	Commander US Army BMD Command ATTN: BDMSC-TFN/N.J. Hurst P.O. Box 1500 Huntsville, AL 35804
2	Deputy Chief of Staff for Operations and Plans ATTN: Technical Library Director of Chemical & Nuc Operations Department of the Army Washington, DC 20310
2	Office, Chief of Engineers Department of the Army ATTN: DAEN-MCE-D DAEN-RDM 890 South Pickett Street Alexandria, VA 22304
3	Commander US Army Engineer Waterways Experiment Station ATTN: Technical Library William Flathau Leo Ingram P.O. Box 631 Vicksburg, MS 39181
1	Commander US Army Engineer School Ft. Belvoir, VA 20060
1	Commander US Army MERADCOM ATTN: DRDME-EM, D. Frink Fort Belvoir, VA 22060
1	Commander US Army Materiel Development and Readiness Command ATTN: DRCDMD-ST 5001 Eisenhower Avenue Alexandria, VA 22333
1	Commander US Army Armament Research and Development Command ATTN: DRDAR-TDC Dover, NJ 07801
3	Commander US Army Armament Research and Development Command ATTN: DRDAR-LCN-F, W. Reiner DRDAR-TSS Dover, NJ 07801
1	Commander US Army Armament Materiel Readiness Command ATTN: DRSAR-LEP-L Rock Island, IL 61299
1	Director US Army ARRADCOM Benet Weapons Laboratory ATTN: DRDAR-LCB-TL Watervliet, NY 12189
1	Commander US Army Aviation Research and Development Command ATTN: DRDAV-E 4300 Goodfellow Boulevard St. Louis, MO 63120

DISTRIBUTION LIST

No. of Copies	Organization
1	Commander US Army Research Office P.O. Box 12211 Research Triangle Park NC 27709
4	Commander US Army Nuclear & Chem Agency ATTN: ACTA-NAW MONA-WE Technical Library MAJ Uecke 7500 Backlick Rd, Bldg. 2073 Springfield, VA 22150
1	Commander US Army TRADOC ATTN: ATCD-SA, Mr. O. Wells Fort Monroe, VA 23651
2	Director US Army TRADOC Systems Analysis Activity ATTN: LTC John Hesse ATAA-SL, Tech Lib White Sands Missile Range NM 88002
1	Commander US Combined Arms Combat Developments Activity ATTN: ATCA-CO, Mr. L. C. Pleger Fort Leavenworth, KS 66027
1	Commandant Interservice Nuclear Weapons School ATTN: Technical Library Kirtland AFB, NM 87115
1	Chief of Naval Material ATTN: MAT 0323 Department of the Navy Arlington, VA 22217
2	Chief of Naval Operations ATTN: OP-03EG OP-985F Department of the Navy Washington, DC 20350
1	Chief of Naval Research ATTN: N. Perrone Department of the Navy Washington, DC 20360
1	Director Strategic Systems Projects Ofc ATTN: NSP-43, Tech Lib Department of the Navy Washington, DC 20360
1	Commander Naval Electronic Systems Com ATTN: PME 117-21A Washington, DC 20360
1	Commander Naval Facilities Engineering Command Washington, DC 20360
1	Commander Naval Sea Systems Command ATTN: ORD-91313 Library Department of the Navy Washington, DC 20362
3	Officer-in-Charge (Code L13) Civil Engineering Laboratory Naval Constr Btn Ctr ATTN: Stan Takahashi R. J. Odello Technical Library Port Hueneme, CA 93041
1	Commander David W. Taylor Naval Ship Research & Development Ctr ATTN: Lib Div, Code 522 Bethesda, MD 20084

DISTRIBUTION LIST

No. of Copies	Organization
1	Commander Naval Surface Weapons Center ATTN: DX-21, Library Br. Dahlgren, VA 22448
2	Commander Naval Surface Weapons Center ATTN: Code WA501/Navy Nuclear Programs Office Code WX21/Tech Lib Silver Spring, MD 20910
1	Commander Naval Weapons Center ATTN: Code 3431, Tech Lib China Lake, CA 93555
1	Commander Naval Weapons Evaluation Fac ATTN: Document Control Kirtland Air Force Base Albuquerque, NM 87117
1	Commander Naval Research Laboratory ATTN: Code 2027, Tech Lib Washington, DC 20375
1	Superintendent Naval Postgraduate School ATTN: Code 2124, Technical Reports Library Monterey, CA 93940
1	AFSC (Tech Lib) Andrews Air Force Base Washington, DC 20331
1	ADTC (DLODL) Eglin AFB, FL 32542
1	AFATL (DLYV) Eglin AFB, FL 32542
1	RADC (EMTLD/Docu Library) Griffiss AFB, NY 13340
1	AFWL/NTES (R. Henny) Kirtland AFB, NM 87115
1	AFWL/NTE, CPT J. Clifford Kirtland AFB, NM 87115
2	Commander-in-Chief Strategic Air Command ATTN: NRI-STINFO Lib Offutt AFB, NB 68113
1	AFIT (Lib Bldg. 640, Area B) Wright-Patterson AFB Ohio 45433
1	FTD (TD/BTA/Lib) Wright-Patterson AFB Ohio 45433
1	Director Lawrence Livermore Lab ATTN: Tech Info Dept L-3 P.O. Box 808 Livermore, CA 94550
1	Director Los Alamos Scientific Lab ATTN: Doc Control for Rpts Lib P.O. Box 1663 Los Alamos, NM 87544
2	Sandia Laboratories ATTN: Doc Control for 3141 Sandia Rpt Collection L. J. Vortman Albuquerque, NM 87115
1	Sandia Laboratories Livermore Laboratory ATTN: Doc Control for Tech Lib P.O. Box 969 Livermore, CA 94550

DISTRIBUTION LIST

No. of Copies	Organization
1	Director National Aeronautics and Space Administration Scientific & Tech Info Fac P.O. Box 8757 Baltimore/Washington International Airport MD 21240
1	Aerospace Corporation ATTN: Tech Info Services P.O. Box 92957 Los Angeles, CA 90009
1	Agbabian Associates ATTN: M. Agbabian 250 North Nash Street El Segundo, CA 90245
1	The BDM Corporation ATTN: Richard Hensley P.O. Box 9274 Albuquerque International Albuquerque, NM 87119
1	The Boeing Company ATTN: Aerospace Library P.O. Box 3707 Seatle, WA 98124
1	Goodyear Aerospace Corp ATTN: R. M. Brown, Bldg 1 Shelter Engineering Litchfield Park, AZ 85340
5	Kaman AviDyne ATTN: Dr. N.P. Hobbs (4 cys) Mr. S. Criscione 83 Second Avenue Northwest Industrial Park Burlington, MA 01830
3	Kaman-Nuclear ATTN: Library P. A. Ellis F. H. Shelton 1500 Garden of the Gods Road Colorado Springs, CO 80907
1	Kaman Sciences Corporation ATTN: Don Sachs Suite 703 2001 Jefferson Davis Highway Arlington, VA 22202
1	Kaman-TEMPO ATTN: DASIAC P.O. Drawer QQ Santa Barbara, CA 93102
1	Kaman-TEMPO ATTN: E. Bryant, Suite UL-1 715 Shamrock Road Bel Air, MD 21014
1	Lockheed Missiles & Space Co. ATTN: J. J. Murphy, Dept. 81-11 Bldg. 154 P.O. Box 504 Sunnyvale, CA 94086
1	Martin Marietta Aerospace Orlando Division ATTN: G. Fotieo P.O. Box 5837 Orlando, FL 32805
2	McDonnell Douglas Astronautics Corporation ATTN: Robert W. Halprin Dr. P. Lewis 5301 Bolsa Avenue Huntington Beach, CA 92647
2	The Mitre Corporation ATTN: Library J. Calligeros, Mail Stop B-150 P.O. Box 208 Bedford, MA 01730
1	Pacific Sierra Research Corp ATTN: Dr. Harold Brode 1456 Cloverfield Boulevard Santa Monica, CA 90404

DISTRIBUTION LIST

No. of Copies	Organization
1	Physics International Corp 2700 Merced Street San Leandro CA 94577
1	Radkowski Associates ATTN: Peter R. Radkowski P.O. Box 5474 Riverside, CA 92517
4	R&D Associates ATTN: Jerry Carpenter J. G. Lewis Technical Library Allan Kuhl P.O. Box 9695 Marina del Rey, CA 90291
1	RCA Government Communications Systems 13-5-2 Front & Copper Sts. Camden, NJ 08102
2	Science Applications, Inc. ATTN: Burton S. Chambers John Cockayne P.O. Box 1303 1710 Goodridge Drive McLean, VA 22102
1	Science Applications, Inc. ATTN: Technical Library P.O. Box 2351 La Jolla, CA 92038
1	Science Systems and Software ATTN: C. E. Needham P.O. Box 8243 Albuquerque, NM 87198
1	Science Systems and Software ATTN: Technical Library P.O. Box 1620 La Jolla, CA 92037
1	TRW Systems Group ATTN: Benjamin Sussholtz One Space Park Redondo Beach, CA 90278
2	Union Carbide Corporation Holifield National Laboratory ATTN: Doc Control for Tech Lib Civil Defense Research Proj P.O. Box X Oak Ridge, TN 37830
1	Weidlinger Assoc. Consulting Engineers ATTN: M. L. Baron 110 East 59th Street New York, NY 10022
1	Battelle Memorial Institute ATTN: Technical Library 505 King Avenue Columbus, OH 43201
1	California Inst of Tech ATTN: T. J. Ahrens 1201 E. California Blvd. Pasadena, CA 91109
2	Denver Reseach Institute University of Denver ATTN: Mr. J. Wisotski Technical Library P.O. Box 10127 Denver, CO 80210
1	IIT Research Institute ATTN: Milton R. Johnson 10 West 35th Street Chicago, IL 60616
1	J. D. Haltiwanger Consulting Services B106a Civil Engineering Bldg. 208 N. Romine Street Urbana, IL 61801

DISTRIBUTION LIST

No. of Copies	Organization
1	Massachusetts Institute of Technology Aeroelastic and Structures Research Laboratory ATTN: Dr. E. A. Witmer Cambridge, MA 02139
2	Southwest Research Institute ATTN: Dr. W. E. Baker A. B. Wenzel 8500 Culebra Road San Antonio, TX 78228
1	SRI International ATTN: Dr. G. R. Abrahamson 333 Ravenswood Avenue Menlo Park, CA 94025
1	Stanford University ATTN: Dr. D. Bershader Durand Laboratory Stanford, CA 94305

No. of Copies	Organization
1	Washington State University Physics Department ATTN: G. R. Fowles Pullman, WA 99164
1	Black & Veatch Engineers and Architects Inc. ATTN: W. V. Hill 7611 State Line Drive Kansas City, MO 64114

Aberdeen Proving Ground

Dir, USAMSAA
ATTN: DRXSY-D
DRXSY-MP, H. Cohen
Cdr. USATECOM
ATTN: DRSTE-TO-F
Dir, USACSL
Bldg. E3516, EA
ATTN: DRDAR-CLB-PA

USER EVALUATION OF REPORT

Please take a few minutes to answer the questions below; tear out this sheet, fold as indicated, staple or tape closed, and place in the mail. Your comments will provide us with information for improving future reports.

1. BRL Report Number ______________________________

2. Does this report satisfy a need? (Comment on purpose, related project, or other area of interest for which report will be used.)

____

____

____

3. How, specifically, is the report being used? (Information source, design data or procedure, management procedure, source of ideas, etc.) ______________________________

____

____

4. Has the information in this report led to any quantitative savings as far as man-hours/contract dollars saved, operating costs avoided, efficiencies achieved, etc.? If so, please elaborate.

____

____

5. General Comments (Indicate what you think should be changed to make this report and future reports of this type more responsive to your needs, more usable, improve readability, etc.) ______________________________

____

____

____

6. If you would like to be contacted by the personnel who prepared this report to raise specific questions or discuss the topic, please fill in the following information.

Name: ______________________________

Telephone Number: ______________________________

Organization Address: ______________________________

____

____

FOLD HERE

Director
US Army Ballistic Research Laboratory
ATTN: DRDAR-BLA-S
Aberdeen Proving Ground, MD 21005

NO POSTAGE
NECESSARY
IF MAILED
IN THE
UNITED STATES

OFFICIAL BUSINESS
PENALTY FOR PRIVATE USE, $300

BUSINESS REPLY MAIL
FIRST CLASS PERMIT NO 12062 WASHINGTON, DC

POSTAGE WILL BE PAID BY DEPARTMENT OF THE ARMY

Director
US Army Ballistic Research Laboratory
ATTN: DRDAR-BLA-S
Aberdeen Proving Ground, MD 21005

FOLD HERE